Fluorescence-based fibre optic arrays: a universal platform for sensing

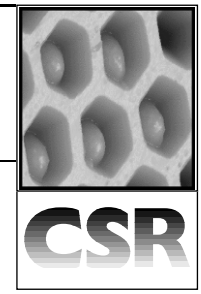

Jason R. Epstein and David R. Walt*

The Max Tishler Laboratory for Organic Chemistry, Department of Chemistry, Tufts University, Medford, Massachusetts 02155

Received 15th January 2003
First published as an Advance Article on the web 14th April 2003

Optical fibres provide a universal sensing platform as they are easily integrated with a multitude of different sensing schemes. Such schemes enable the preparation of a multitude of sensors from relatively straightforward pH sensors, to more complex ones, including artificial olfaction sensors, high-density oligonucleotide arrays, and high-throughput cell-based arrays. Imaging fibre bundles comprised of thousands of fused optical fibres are the basis for an optically connected, individually addressable parallel sensing platform. Fibre optic imaging bundles possess miniature feature sizes (3–10 micron diameter fibres), allowing high-density sensor packing ($\sim 2 \times 10^7$ sensors per cm^2). Imaging fibre bundles transmit coherent images enabling combined imaging and sensing, relating the responses monitored by the sensor to observable physical changes. The individual fibre cores can also be selectively etched to form a high-density microwell array capable of housing complementary sized microsensors. The miniature feature sizes facilitate a faster response and more sensitive measurement capabilities. The platform is extremely versatile in its sensing design, allowing the sensing scheme to be tailored to fit the experimental design, whether for monitoring single analytes or more complex multiplexed assays. A number of sensing schemes and applications are described in this review.

1 Optical fibres

Optical fibres consist of a glass or plastic core surrounded by a clad material of lower refractive index. Based on the difference in refractive indices, light is reflected at the core-clad interface (Figure 1). Light propagates through the fibre core and is

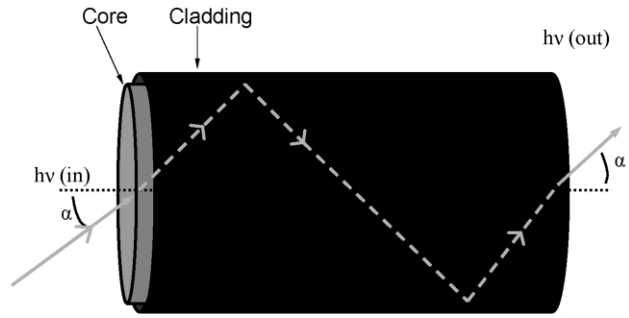

Fig. 1 Schematic of an optical fibre. Light propagates in the fibre along the entire length due to the refractive index differences of the core and clad materials.

transmitted the length of the fibre with minimal attenuation. As such, optical fibres are an ideal platform for sensing as they enable light to be carried over long distances. Conveying a

Jason R. Epstein received his Bachelor's degree from Siena College in 1992 and his Master's degree from Portland State University in 1999. From 1992–97, Jason was employed at Cambridge Isotope Laboratories as a process chemist. He is currently working towards his PhD in chemistry/biotechnology in the laboratory of David Walt at Tufts University. His main research focus concerns practical applications for fiber optic microsphere-based oligonucleotide microarrays.

Jason R. Epstein

David R. Walt is Robinson Professor of Chemistry at Tufts University. He received a BS in Chemistry from the University of Michigan and a PhD in Chemical Biology from SUNY at Stony Brook. After postdoctoral studies at MIT, he joined the chemistry faculty at Tufts. Professor Walt served as Chemistry Department Chairman from 1989 to 1996. Dr Walt serves on many government advisory panels and boards. He is Executive Editor of Applied Biochemistry and Biotechnology and serves on the editorial advisory board for numerous journals. Dr Walt is the Scientific Founder of Illumina, Inc. He has received numerous national and international awards and honors recognizing his work and is a fellow of the American Association for the Advancement of Science. His research interests are in the fields of sensors, biosensors, micro and nanoarrays, artificial olfaction, and functional screening.

David R. Walt

This journal is © The Royal Society of Chemistry 2003

signal over long distances allows optical fibres to be used in remote or hazardous sensing applications that typically cannot be addressed with other analytical techniques. Fluorescence-based methods are particularly amenable to fibre optic platforms. For fluorescence-based sensing, excitation light is delivered through the fibre to a fluorescent indicator attached to the fibre's distal end, and the resulting isotropic fluorescence emission is transmitted back through the fibre to a detector. Fluorescence-based sensing techniques are versatile, enabling interrogation of multiple optical properties simultaneously, including excitation and/or emission wavelengths, emission intensity, and fluorescence lifetime. Fluorescence assays can be readily multiplexed by simultaneously using multiple indicators reporting at different wavelengths. Multiplexed fluorescence-based fibre optic sensors have been applied to the detection of ions and organic compounds, as well as numerous biological compounds.[1,2]

The desire for parallel interrogation and high throughput analysis has prompted the development of sensor array platforms. Imaging fibre bundles are already formatted into an array, composed of thousands of single core fibres coherently fused, with each fibre in the bundle maintaining its own independent light pathway (Figure 2). A fibre bundle with 3.0

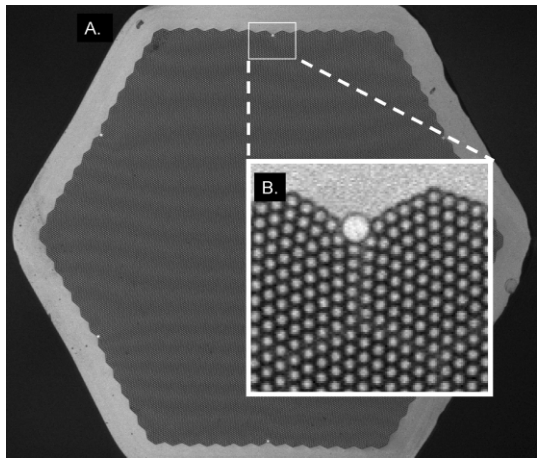

Fig. 2 An image of a 1 mm^2 fiber bundle containing ~50,000 total 3 micron individual fibres. A) An entire hexagonally packed bundle. B) A higher magnification of the fiber bundle showing the miniature feature sizes and close-packed arrangement. The large circle is a positional marker built into the array.

μm diameter cores and an overall 1 mm bundle diameter contains over 50,000 individual fibres. More flexible bundles with smaller diameters and smaller numbers of total fibres are also available. The small dimensions and close packing arrangement associated with optical fibre bundles account for their use as high-density sensor arrays. Imaging fibres are aptly suited for use as sensor arrays, enabling rapid, simultaneous analysis of complex mixtures.

2 Optical fibre-based sensors

The work described in this review employs fluorescence as the signal transduction method for optical fibre-based sensing. This review highlights the advantages of the fibre optic platform for fluorescence-based sensing, including their miniature sensor size, high sensitivity, high throughput, and versatility. The next two sections describe both the general instrumentation and common sensor fabrication methods, including the various approaches for attaching the requisite sensing chemistry to optical fibres. Subsequent sections describe optical fibre-based sensor applications. While the fibre optic platform described in this review employs imaging bundles as the substrate, the fundamental sensing chemistries were initially developed for single core fibre optic sensors and therefore, they will be mentioned briefly in several sections.

2.1 Fluorescence imaging systems

Although each type of fibre optic sensor requires specific instrumentation, there are some common system components for all fluorescence-based sensing systems (Figure 3). An

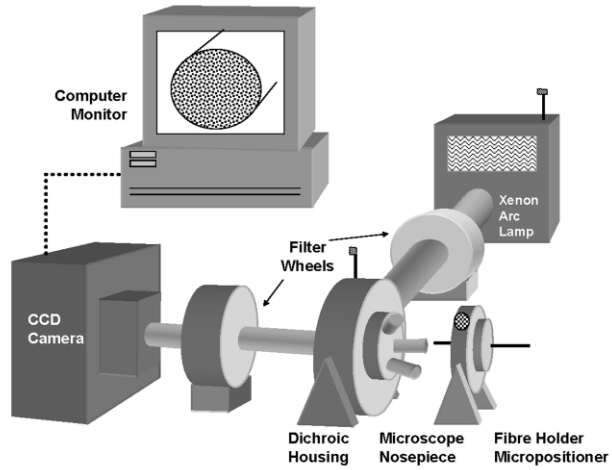

Fig. 3 The general setup of the custom-built imaging systems consisting of a computer-controlled modified epifluorescence microscope.

excitation light source, such as a laser, light emitting diode, or white light source, is used to excite the fluorescent indicator. In many research applications, a white light source, such as a xenon arc lamp, is filtered through an excitation filter to provide monochromatic light. A white light source is extremely flexible, as it can excite fluorophores over the entire visible spectrum, which enables an extensive range of fluorescent dyes to be used. Excitation light entering the fibre is collimated and focused at the fibre's proximal end and transmitted to the sensing material located at the fibre's distal tip. Light emitted from the fluorophore is captured and carried back through the fibre. After exiting the proximal end, the light is filtered and projected onto a charge-coupled device (CCD) camera. The recorded intensities are proportional to the fluorescence at each individual fibre position. Modern cameras have CCD chips with megapixel resolution. High resolution is necessary to differentiate an imaging fibre's miniature feature sizes (3 μm). CCD cameras provide high quantum efficiencies and low dark current noise, which optimises the signal-to-noise ratio. The low dark current enables longer acquisition times without a significant noise increase. By employing a less intense light source in tandem with a CCD camera, photobleaching associated with laser excitation is limited, without sacrificing the detection capabilities. In addition, laser excitation sources can be expensive and have fixed excitation bandwidths. A computer-controlled system can use scripted programs to allow rapid transfer between wavelengths and filter sets. This rapid transfer ability enables multiple wavelengths to be used for real-time analysis of multiple fluorescent indicators.

3 Sensor fabrication methods

Sensors were fabricated by attaching the sensing chemistries to the fibre optic microarray platform using three general approaches: homogenous sensor/polymer layers, discrete polymeric sensing regions, and microsphere-based sensors. The three sensor fabrication approaches vary in their complexity and

provide different levels of parallel interrogation. The extent of parallel interrogation depends on the sensing region dimensions, with the smallest feature corresponding to a single fibre in the bundle.

3.1 Polymer sensing layers

The first sensing format involves coating the entire distal fibre face with a sensing layer. The sensor is comprised of a specific indicator chemistry attached to a polymer layer. The sensing layer is attached directly to the fibre, forming a thin polymer film (from 5 to 100 μm) so it remains optically transparent.

To attach the sensing layer to the fibre, the glass fibre surface is first derivatized to incorporate functional groups compatible with the polymer. For example, fibres can be treated with 3-(trimethoxysilyl)propyl methacrylate for copolymerisation into a methacrylate polymer matrix.[3] The surface-derivatized fibre is then coupled to the sensing layer by two different methods: photoinitiation or dip coating polymerisation. Photoinitiation entails immersing the fibre in a prepolymer solution containing monomer, initiator, crosslinker, and indicator, and then initiating polymerisation by delivering light through the fibre to the fibre's distal face. In this method, polymer forms directly on the fibre surface while the bulk solution remains unpolymerised. Dip coating the fibre involves immersing the pre-functionalised fibre into a prepolymer/indicator solution. When the fibre is removed from the prepolymer, the polymer coating formed on the fibre surface functions as the sensing layer. In either case, all polymerised sensing regions produce a uniform distribution of indicator, as determined by visualization of the fluorescence intensity on the fibre face.

Polymerisation of a sensing layer on a single core fibre allows only a single parameter to be measured. When an imaging fibre bundle is coated with a uniform sensing layer, each individual fibre in the bundle acts as an independently addressable sensor, providing an array of sensors. With both single core fibres and imaging arrays, the sensing film thickness influences the sensor response time.

3.2 Discrete polymer sensors

A second sensor fabrication technique involves polymerising discrete sensing regions at specific locations on the fibre face. This method allows multiple sensors to be immobilized on a single fibre array. The sensing regions are fabricated using chemistry identical to the photoinitiated polymer coating sensors described above. Multiple polymeric sensing regions are fabricated on the same fibre, with each single sensor region having dimensions between 20–100 microns in diameter (Figure 4). Different sensor regions are created via the photoinitiation light focused to discrete areas on the fibre's proximal end. Only the areas exposed to the photoinitiation light form a photopolymer on the distal fibre face. By exposing separate regions of the fibre face to different photopolymers, different sensing chemistries can be incorporated onto a single imaging bundle. While this format enables multiple sensing regions to be addressed in parallel, the total number of unique sensors that can be assembled on a single fibre is limited because the individual sensor sizes are relatively large as they encompass multiple fibres.

3.3 Microwell arrays

Fibre optic bundles also serve as a platform for a high density ordered microwell array.[4] This sensor fabrication method addresses the need for higher levels of parallel sensing and high throughput analysis. Microwells are formed based on the

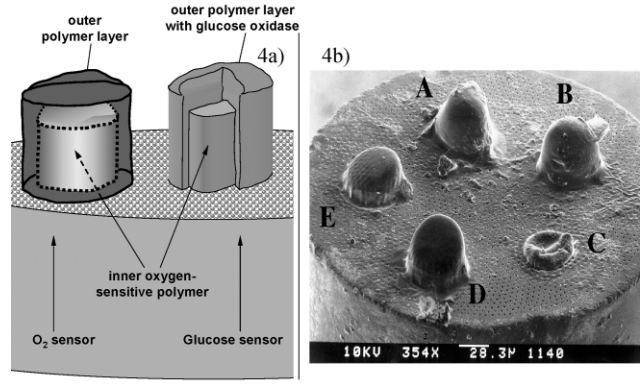

Fig. 4 a) Schematic diagram of the discrete glucose sensing regions. The inner polymer contains the oxygen sensitive indicator. One outer polymer coating is doped with glucose oxidase. 4b) Scanning electron micrograph of the triple sensor CO_2(A and B), pH (C), and O_2(D and E). The pH sensor collapsed due to water evaporation when subjected to high vacuum during the gold coating process. Reprinted from "Simultaneous monitoring of pH, CO_2, and O_2 using an optical imaging fiber", J. A. Ferguson *et al*., *Anal Chim. Acta*, 1997, **340**, 123, © 1997 with permission from Elsevier Science.

compositional differences between the core and clad materials, which allow the cores to be selectively etched, forming a patterned array of wells (Figure 5). The microwells have

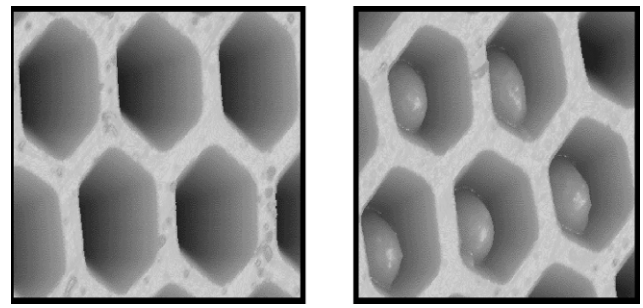

Fig. 5 Atomic force micrographs of etched fibre bundles (left). Each well is 3 microns in diameter. The wells can be filled with complementary-sized microspheres derivatized with different sensing chemistries (right).

diameters equal to those of the cores from which they were formed, with the relative depths dependant on the fibre composition, etchant concentration, and exposure time. These wells can be loaded with complementary-sized microspheres containing a variety of incorporated sensing materials. The microsphere sensors consist of silica or polymeric microparticles containing fluorescent indicators or derivatized with specific recognition elements, such as single stranded oligonucleotides. The fibre core diameters and microwell depths can be tailored to complement a variety of sensing materials. In addition to microspheres, individual cells have been employed as sensing materials. For cell-based sensing, a number of different cell types can be loaded onto arrays, including yeast (*Saccharomyces cerevisiae*),[5] bacteria (*Escherichia coli*),[5] and mouse fibroblast cells.[6] Some cell types can be genetically modified, offering more flexibility in sensor design. The genetic modifications make available indicating cells that respond to their environment. Cell-based sensor arrays are described in more detail below in the biosensors and biomonitoring section. In either microsphere or cell-based arrays, multiple sensor types can be added to the etched fibre face to form the array. When the arrays are fabricated, the sensor addition process is random, so sensor placement is unknown. After fabrication, the random array requires a registration process such that the positions of each sensor in the array can be determined. Sensor array decoding schemes are described in the next section. The random self-assembly process dictates that sensor arrays are formed

with multiple replicates of each sensor type to ensure representation, which also provides a signal averaging benefit. Signal averaging of many identical sensors, increases the total signal-to-noise ratio by the square root of the number of sensors examined. In addition, replicate sensors in the array minimize potential false positive and false negative signals by confirming the signal response. The simple sensor fabrication protocol and miniature sensor size allow enormous numbers of sensor arrays to be made at one time. A single batch of sensors is enough to fabricate thousands of arrays; one millilitre of sensor stock contains 10 billion identical microsphere sensors so that it is easy to fabricate arrays with identical sensing behaviour.

The miniature sensor feature size also directly affects the sensor packing density, sensitivity and experimental throughput of the resulting array. Higher packing density results in smaller overall array sizes and interrogation of small sample volumes. The same number of target molecules in a smaller volume yields a higher local concentration, making it possible to detect a small absolute number of molecules.

3.3.1 Array decoding. The array self-assembly process results in sensors randomly dispersed into the microwells, so an optical decoding system is required.[7–9] To ascertain the position of multiple sensor types in a randomised array, the sensing elements are encoded with fluorescent dyes prior to array fabrication. Sensor encoding links each specific sensor type with a unique fluorescent indicator pattern. Encoding dyes must have emission spectra separate from those of the indicators used for sensing. By employing multiple fluorescent dyes with multiple dye intensities, hundreds of different microsphere sensor types can be encoded with different optical "bar codes".

The encoding dyes can be incorporated into the microspheres via three different methods: adsorption, covalent attachment, or internal entrapment. Adsorption methods are dependant on the microsphere compositions and surface functionality, as well as the dye's structure. Covalent attachment requires compatible functional groups between the microsphere and dye, which can be used to link the two species. Internally trapped dyes are introduced into polymeric microspheres in the presence of organic solvents. The solvents swell the polymer, allowing the dye to penetrate into the particle interior. Upon solvent evaporation, the dye is trapped in the polymeric matrix. In this method, it is important that the encoding dyes are insoluble in the solvent in which the measurements are to be performed.

4 Applications

Imaging fibre bundles are an ideal platform for multiplexing because they contain thousands of individually addressable light pathways. Each fibre is aligned with a spatially discrete sensing region that can be used in a sensor array format. In this fashion, every sensing region in the bundle can be interrogated simultaneously. The sensor microarrays are used in numerous applications, described in the following sections.

4.1 Combined imaging and sensing

Imaging fibre sensor arrays can be used for combined imaging and sensing. In this application, a sensing layer is coated uniformly onto the fibre's distal tip. A thin polymer coating is deposited so that light can still be transmitted readily through the sensing layer. Each fibre transmits a signal originating from the sensing region at its distal tip. When imaging bundles are used to transmit images, each fibre conveys a small part of the image. The coherent nature of the bundle enables the individual fibre pixels to be assembled into an entire image (Figure 6). The

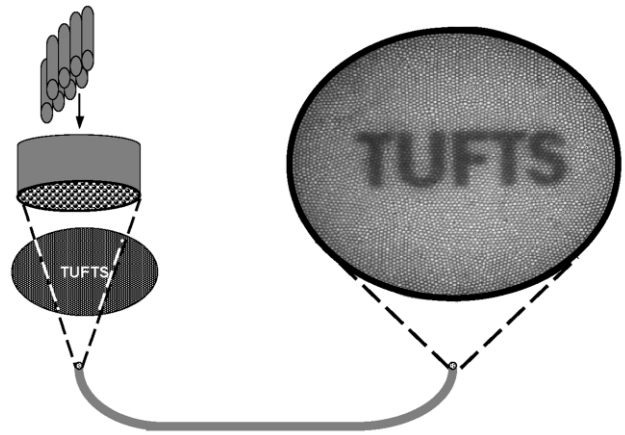

Fig. 6 Coherent imaging bundles. Fibre optic imaging bundles are comprised of fused single core fibres. Thousands of individual 3 micron fibres can be bundles in a 500 micron diameter bundle. The bundles can be used to transmit an image, where each individual fibre in the bundle acts as a single pixel of the image.

imaging system is capable of switching between white light and a specific indicator wavelength. Because each fibre conveys both white light and a fluorescent signal originating from the sensing layer, a fibre optic bundle can be used for both imaging and sensing. Imaging fibres used in white light mode can be used to visualize samples and to control sensor placement, while the appropriate excitation and emission wavelengths can be used to interrogate the immobilized indicator. Employing an imaging bundle to visualize the changes links the physical changes with the fluorescent intensity measurements. A major advantage with this approach is that no exogenous indicator is added to the solution providing for relatively unperturbed measurements. The spatial resolution is determined by the individual fibre's pixel size and can be less than one micron.

Combined imaging and sensing was performed on live cells.[10] Sea urchin eggs, upon fertilization, undergo a Na^+/H^+ exchange with their environment. This cation exchange mechanism releases H^+ from the cell, forming a pH gradient to prevent additional sperm from reaching the egg. This fibre optic sensor array was coated with a pH sensitive polymer layer to monitor local pH changes while simultaneously visualizing structural changes, including cell division. The pH sensitive fluorescent indicator seminaphthofluorescein (SNAFL) was covalently attached to the polymer layer. Fluorescein and its derivatives, such as SNAFL, have both acid and base forms with separate excitation wavelengths (440 nm/490 nm, respectively), but a single emission wavelength (530 nm). The acid form of fluorescein has minimal fluorescence but its conjugate base strongly fluoresces, so a ratiometric measurement of the base and acid intensities (490/440) could be used to avoid sensor drift. The imaging system was programmed to enable both excitation wavelengths to be measured continuously. Within a minute of sperm addition, the fluorescence intensity increased dramatically, and cell division was observed. This platform is capable of monitoring multiple cells simultaneously at physiological conditions, without compromising the cell membrane.

4.1.1 Corrosion monitoring. Corrosion was also monitored with a fibre optic pH sensor.[11,12] The sensor array was brought proximal to a metal surface, to measure the release of H^+ from discrete regions on the surface where corrosion took place. Localized corrosion was measured while white light images of the damaged areas of the corrosion surface were viewed simultaneously. Imaging fibre sensors were employed to monitor crevice, pitting, and galvanic corrosion. By simultaneously measuring and visualizing corrosion patterns, information related to corrosion rates and inhibition processes could be obtained. Fluorescence intensity changes were observed, signalled by a pH sensitive dye response (fluorescein iso-

thiocyanate, FITC) to the electrochemical generation of local H^+ or OH^- concentrations. H^+ ions were formed at the anode due to solvolysis of the anodic metal, and OH^- was formed at the cathode based on the reduction of water and/or oxygen. Areas with large fluorescence intensity changes were imaged with a fibre positioned a few microns from the metal surface, and ratiometric fluorescence measurements were performed. The fluorescent responses were confirmed by surface imaging with atomic force microscopy (AFM) to map topographic changes.

Corrosion sites were monitored for the formation and passivation of crevices and corrosive pitting.[11] Metals such as iron and nickel are oxidized in the presence of chloride ions, resulting in pH changes. A stainless steel surface was immersed in 0.1 M KCl (pH 6.6) and subjected to a potential of +0.5 V vs. saturated calomel electrode. Deviations from the background pH were seen concomitant with visualized narrow fissures. Regions of increased fluorescent intensity correlated with circular craters 10–20 μm in diameter. These crevices and pit regions were indicative of localized corrosion (Figure 7).

Fig. 7 Image monitoring pH after 20 minutes of an optical fibre pH sensor array over an aluminium surface. Darker regions correspond to areas of lower pH. Reprinted with permission from S. Szunerits and D. R. Walt, *Anal. Chem.*, 2002, **74**, 886. © 2002 American Chemical Society.

Corrosion was also viewed with the Cu/Al galvanic pair in slightly acidic media. In this case, the reduced species was again oxygen/water, but Al metal was now being oxidized. The applied constant anodic potential was +0.2 to +0.5 V. The measured fluorescence changes were proportional to the applied potential. Higher buffer concentrations were more damaging to the surface, corroborated by the rougher surfaces viewed in the AFM images. The same galvanic pair was used to visualize the effects of corrosion with different indicators.[12] SNAFL was covalently attached to the polymer matrix and a constant anodic potential (0.4 V) was applied. Fluorescence intensity decreases were seen due to decreases in pH, similar to those seen with FITC. Areas of marked pH differences were observed, followed by a return to the buffer pH value indicative of surface passivation. The extent of corrosion was also monitored with an aluminium sensitive indicator, morin, which results in a substantial fluorescence increase when complexed with Al^{+3}. Initially, morin was used free in solution, but it was also immobilized to the polymer layer along with a pH sensitive dye. Immobilizing the morin improved the ability to monitor the spatial and temporal corrosion effects. The sensor provided a linear kinetic corrosion profile for concentrations of 0.5–5.0 mM, and was reusable for over 100 assays. Two known corrosion inhibitors were also investigated, $CeCl_3$ and 8-hydroxyquinone (8HQ). Inhibitors would be expected to show decreases in current and smaller areas of active corrosion, indicative of surface passivation. For example, $CeCl_3$ adsorbs to the surface, forming a metal oxide passivation layer. At 3.0 mM $CeCl_3$, the current decreased from 50 to 20 μA within one minute, resulting in lower measured pH changes (0.4 pH units as compared to 0.9 uninhibited). In addition, corrosion sites were observed to be approximately half the size as those formed without inhibitors present. The 8HQ also inhibits corrosion of aluminium and demonstrated substantially better inhibition qualities than $CeCl_3$. Active corrosion sites were 1/10 the size of corrosion sites observed without the inhibitor, and the pH change decreased to 0.15 units versus the 0.9 unit decrease observed in the solution without inhibitor. With 8HQ, the entire surface was passivated within 20 minutes.

4.2 High-density discrete sensing regions

An improved method for preparing discrete photodeposited sensing regions could be performed by employing the individual fibre pixels as the pathways for photoinitiation.[13] Whereas the previously described methods used photoinitiation light focused onto the fibre face, an improved photoinitiation method was developed that directed photoinitiation light through the fibre itself.[14] Building off of this methodology, thousands of oxygen and pH sensors were formed in parallel, each precisely aligned with an individually addressable fibre[13] (Figure 8). The polymerisation process was similar to that

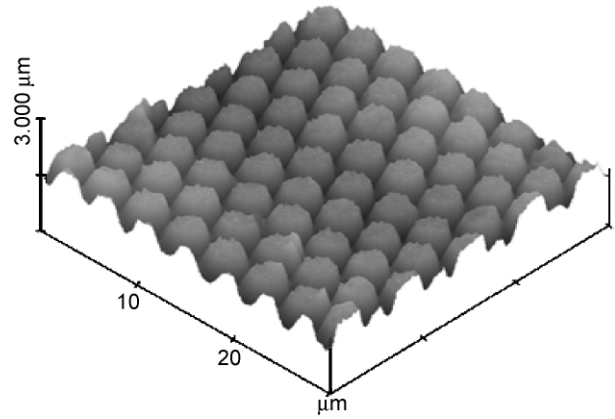

Fig. 8 Atomic force micrograph of a polymer layer pattern from a chemically-etched imaging fiber. Polymerization was initiated with light traveling through the fibre bundle, resulting in an array of 3 micron diameter polymer sensor spots. Reprinted with permission from B. G. Healey and D. R. Walt, *Anal. Chem.*, 1997, **69**, 2213. © 1997 American Chemical Society.

described previously, except the photoinitiation system provided more control over the light intensity and exposure time. The polymerised sensing regions had dimensions of 2.8 μm diameter, with 0.6 μm and 1.2 μm heights for pH and oxygen regions respectively. The pH and O_2 sensors are described in detail in section 4.4. A principal advantage of this method is the hemispherical shape of the miniature sensing regions, which enable radial diffusion, and a more rapid sensor response time. The pH sensor responded to a difference of 1.5 pH units within 300 milliseconds, and the oxygen sensor measured a 90% change from its steady state value in less than 200 milliseconds.

4.3 Artificial olfaction

Traditional sensing approaches require one sensor for every analyte. As the number of analytes to be measured increases, the

array becomes more complex and the possibility for interference grows. An alternative sensing approach is based on principles derived from the mammalian olfactory system. Vertebrate olfaction is known to be both highly sensitive and broadly responsive to a wide range of odours. Rather than utilizing specific receptors for each different analyte, a broad assortment of odours can be sensed using cross-reactive sensor responses. Odours are defined by both their spatial and temporal patterns generated by olfactory receptors and interpreted by the neural circuitry.[15] Similar spatial and temporal responses can be generated with artificial sensory systems, mimicking the cross-reactive nature and neural networking associated with olfaction.

Fluorescence-based fibre optic sensor arrays have been developed, modelled after these olfaction principles.[3, 16–22] Semi-selective, cross-reactive sensors were fabricated to imitate the broad responses of the vertebrate olfactory receptors.[16,19] The functionally diverse sensors were incorporated into polymer matrices on single core fibres as previously described. Bundling multiple single core fibres allowed multiple sensor types to be interrogated simultaneously. This platform provided a simple fabrication protocol, rapid response and low detection limits. Other artificial olfaction systems have been developed[23] using a variety of sensing methods, including conductive polymer,[24,25] surface-acoustic wave,[26,27] and electrochemical schemes.[28,29] Many of these techniques suffer from poor sensor reproducibility, low sensitivity, and slow sensor response.

For the fibre-optic artificial olfaction system, the sensors are comprised of a solvatochromic dye indicator immobilized in a variety of polymers. Solvatochromic dyes shift their fluorescence emission spectrum based on their local environment. The most common solvatochromic dyes red-shift their emission spectrum as polarity increases. Changes in the fluorescence emission spectrum, in turn, affect the quantum efficiency, spectral shape, fluorescence lifetime and the wavelength maximum of the indicator. Each of these optical properties can be simultaneously measured with the fibre optic imaging system. Figure 9 shows fluorescence emission spectra from a dye immobilized in a polymer and exposed to different organic vapours. As can be seen, the more polar the vapour, the more red-shifted is the emission spectrum. The dye's initial microenvironment is defined by the polymer's polarity.[16,17] The analyte vapour diffuses into the polymer layer, influenced by

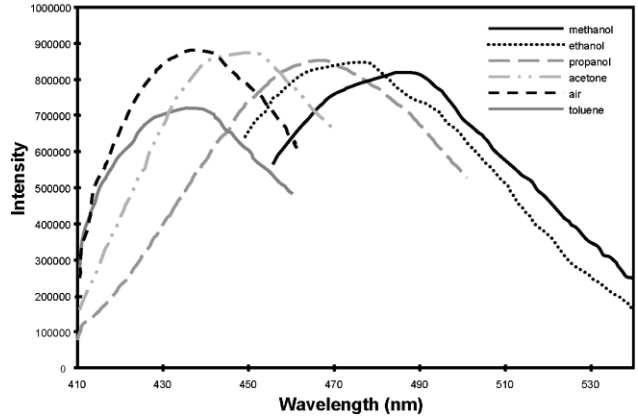

Fig. 9 The solvatochromic effect. Fluorescence emission spectra of a single dye immobilized in a polymer and exposed to different organic vapors. The spectra get more red-shifted with increasing polarity of the vapor.

polymer swelling, hydrophobicity, and adsorption efficiency. By incorporating the same dye into multiple polymers with different polarities, a distinct response pattern is generated for each analyte. Upon exposure to a vapour pulse, vapour diffuses into the polymer and changes its polarity. This polarity change is reported by the solvatochromic dye. Because different vapours diffuse into the polymers at different rates, the temporal responses of the different sensors in the arrays are monitored. To illustrate the different sensor responses, Figure 10 shows the responses of four different sensors exposed to four different analyte vapours. These responses are measured at a single wavelength.

The first generation of fibre optic artificial olfaction employed 300 μm diameter single core fibres coated with different polymer layers to trap the dye Nile Red.[3,16] Nineteen different fibres were bundled to form an array. The advantage of Nile Red as an indicator is that it is soluble in numerous solvents and is relatively photostable. Experiments were performed using the array to discriminate various organic compounds (alcohols, esters, aromatics, etc.), as well as mixtures and concentrations. For each analyte, the different sensors varied in their temporal response shape. Artificial neural networks were trained to detect and identify each analyte. Although identification was not correct 100% of the time, a high degree of differentiation was

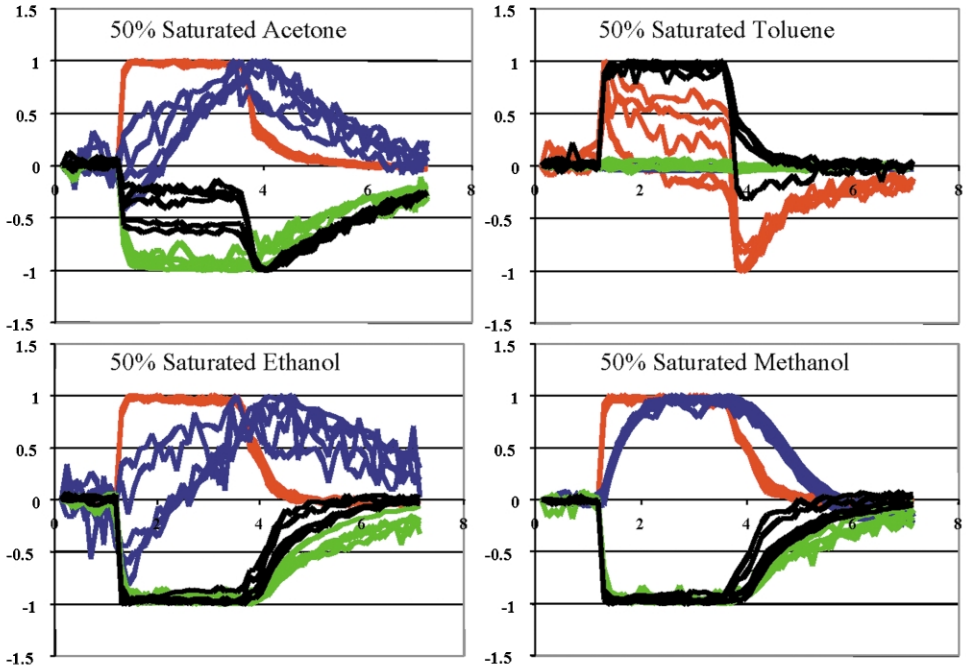

Fig. 10 Four different sensors and their response to four analytes, plotted as normalized fluorescent intensity versus time (s). Note: These responses are monitored at a single wavelength.

observed, and analytes could be detected at concentrations down to 1000 ppm.[3] The array demonstrated millisecond response times. The sensors were stable for weeks and over hundreds of trials. Successful analyte classification from optimised neural networks trained on the temporal responses provided substantial improvement over those generated from integrated fluorescent signals demonstrating the value of using dynamic responses rather than equilibrium values.[16]

Similar experiments were performed using a more advanced classifying algorithm.[18] A learning vector algorithm proved to be more appropriate for pattern recognition applications and provided more reliable analyte classification. The experiments addressed a larger, more diverse pool of analytes and mixtures. Sensor responses were pre-screened to eliminate sensors with minimal responses. A total of 12 sensor-types were employed for 20 analyte vapours. Corrections were made for humidity differences, and responses were normalized to remove concentration dependent effects. A series of descriptors, such as slopes, maximum intensity changes, and average intensity values per unit time, were used in the algorithm. Discrimination and quantification of training sets and external prediction sets were improved over the initial results, approaching 100% classification.

4.3.1 High-density microsphere-based artificial olfaction. While initial artificial olfaction research incorporated discrete polymeric sensing regions, the contemporary design has supplanted the various sensor types with 3 μm fluorescently dyed microspheres.[19–22] Different microsphere compositions perform similar to the polymer layers, providing unique microenvironments for the dye and analyte vapour to interact. By employing microspheres composed of different materials, such as silica or a variety of polymers with different surface and internal functionality, a diverse sensor stock was made. Sensors are randomly distributed into the microwell array, and the response of each microsphere/indicator combination to a particular vapour is used for positional registration. Sensor placement, although random, is easily determined and linked with its response. In this fashion, the dye serves two purposes and the microsensors are termed "self-encoding". The random sensor distribution more closely mimics that of the olfactory epithelium, where primary odour receptor cells are randomly distributed.[30]

The introduction of self-encoded microsphere sensors has revolutionized fibre optic artificial olfaction.[19–22] The miniature sensor feature size provides a more rapid response and higher sensitivity. Miniature sensors provide more surface area for vapour interactions. Micro-sensors also allow a greater sensor packing density compared to other platforms. The sensor loading capacity along with the array fabrication method provides inherent sensor redundancy similar to vertebrate olfaction systems. This redundancy provides a signal to noise amplification that increases as $n^{1/2}$, where n is the number of sensors examined. The positive signal effect is illustrated in Figure 11. Figure 11(a) shows the responses of 39 individual microsensors compared to their summed response. Figure 11(b) illustrates the noise associated with a single microsensor versus the average response of 39 sensors. Array detection limits are determined by taking advantage of signal averaging. Averaging the 39 identical microsensors afforded a sixfold enhancement in signal-to-noise ratio compared to a single sensor, comparable to the theoretical value. A toluene sample (840 ppb, 0.002% in air) was readily detected with signal-summing microspheres, but was undetectable for any single microsensor. Separate arrays were examined months apart, but still maintained their characteristic responses.[19]

These microsphere-based arrays have been applied to the detection of volatile organic compounds (VOC), nitroaromatic explosives-like materials (NAC) and complex mixtures. Self-encoded microsphere-based arrays were fabricated containing equal distributions of six different microsensor types, with approximately 2500 microsensors in total.[20] Analytes included three varieties of coffee beans, acetone, toluene, and 1,3-dinitrobenzene. A classification rate of 100% was obtained for the samples using discriminant function analysis algorithms. Experiments were also performed using specific sensors determined to be effective for detecting explosives-like compounds.[21] The NACs were hidden in complex background vapours at much higher concentrations (10^5 times) to simulate more realistic detection situations. The array provided strikingly different response profiles for such compounds as 4-nitrotoluene, 2,4-dinitrotoluene and 1,3 dinitrobenzene. The

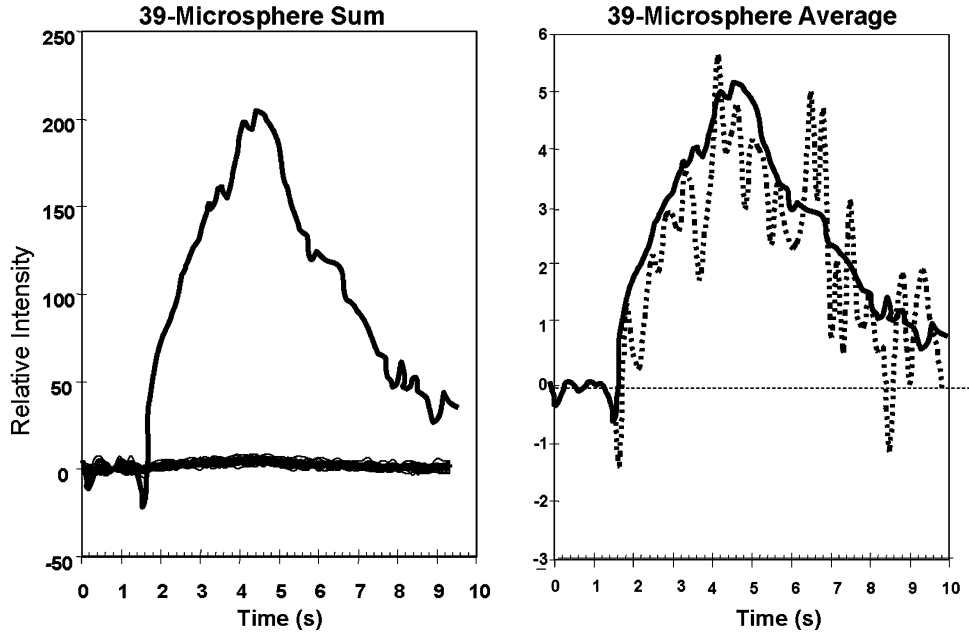

Fig. 11 Signal amplification through microsphere summing—response to 1% methanol vapor in air. Summation of 39 microsphere responses versus the individual microsphere responses (left). The average of the 39 microsphere responses (right). The dotted trace is a single arbitrary microsphere response scaled for comparison and showing how the noise can be virtually eliminated by summing. Reprinted with permission from T. A. Dickinson et al., *Anal. Chem.*, 1999, **71**, 2192. © 1999 American Chemical Society.

characteristic response patterns were retained with sample concentrations between 5 ppb–215 ppm. At these levels of analyte, the detection capabilities are affected more by vapour delivery than by the sensor sensitivity.

The microsphere sensor technology has also improved array-to-array reproducibility.[22] The problem with all previous artificial olfaction arrays is that they eventually lose their ability to respond, resulting in a need to retrain the classifier on the next array. The lack of array reproducibility is partially due to inherent batch-to-batch differences in the fabrication of polymer-based sensors. To counteract this problem, billions of identical microsphere-based sensors are fabricated simultaneously, providing a more homogeneous sensor stock. For analysing multiple arrays fabricated from a single sensor stock, a flexible classifying algorithm was employed to account for minor differences in the response features that affect sensor reproducibility. The classifier corrected for sensor artefacts and assigned values for the discrimination confidence level. In an analytical challenge to detect low-level NACs, different arrays have demonstrated high reproducibility and transfer of a trained classifier across arrays. The ability to transfer the training from array-to-array allows entire arrays to be replaced without retraining, and moves the system towards a database of learned responses similar to odour memory.

4.4 Biosensors and biomonitoring

Biosensors contain a biological recognition element that converts a binding or catalytic event into a detectable signal. As an example, it is possible to prepare a sensor for acetylcholine using the enzyme acetylcholinesterase. In this approach, acetylcholinesterase catalyses the hydrolysis of acetylcholine to choline and acetic acid. The resulting acid can be detected readily by a pH indicator located proximal to the enzyme. An optical sensor for acetylcholine was fabricated by copolymerising a pH sensitive dye and the enzyme into a polymer coating on the distal face of an imaging fibre bundle.[31] Acetylcholineesterase was co-immobilized with fluorescein isothiocyanate (FITC) into a poly-(acrylamide-*co*-*N*-acryloxysuccinimide) matrix on the imaging fibre face. The residual amine and *N*-hydroxysuccinimide ester groups in the polymer react with the FITC and surface lysine residues of the esterase, respectively. Ratiometric fluorescein-based measurements were employed as described above. Sensor response depends on substrate diffusion into the polymer matrix; the acetylcholine sensor provided a rapid (<1 second) response to physiologically significant analyte concentrations.

A similar biosensor was fabricated using the discrete sensing region approach, where dual sensors for pH and penicillin monitoring are fabricated on the same fibre bundle.[32] The enzyme penicillinase, which converts penicillin to penicilloic acid, was co-immobilized with a fluorescein derivative in a discrete polymer region on the fibre face. As the enzyme converted penicillin to penicilloic acid, the pH decreased, resulting in a fluorescence intensity decrease that is monitored via ratiometric fluorescein measurements. The penicillinase was incorporated into the polymer matrix as lyophilised micrometer sized enzyme particles. Upon hydration of the matrix, the enzyme activity was restored. The sensor demonstrated sub-millimolar detection limits for penicillin. Because this sensor responds to both a change in penicillin concentration as well as a pH change, it is necessary to control the pH of the solution being measured. Alternatively, by including a separate pH-sensing region to independently determine the solution pH, measurements of more complex environments where the pH changes over time were possible. This biosensor scheme can be adapted to any other enzyme-based method that generates or consumes protons.

An optical biosensor for combined oxygen and glucose sensing was also fabricated with discrete photopolymerised regions.[33] This dual sensor was fabricated via successive rounds of photopolymerisation. The oxygen-sensing region consisted of an initial 27 μm diameter polymer spot, coated with a second 54 μm diameter polymer layer (Figure 4a). The inner polymer region was embedded with an oxygen sensitive ruthenium(II) dye [both tris(2,2′-bipyridyl ruthenium(II) chloride) and tris(phenanthroline ruthenium(II) chloride) were used] and subsequently coated with a second gas permeable polymer layer containing glucose oxidase. The glucose oxidase reaction consumes oxygen. A decrease in oxygen concentration results in increased fluorescence intensity from the interior ruthenium indicator. The fluorescent signal was dependent on both glucose and oxygen concentrations, therefore the glucose sensors were used in combination with oxygen sensors that measured the solution oxygen concentration, analogous to the dual sensor described above. The sensor's dynamic range was dependent on the amount of enzyme incorporated in the second polymerisation step, and could be tailored to suit a variety of glucose concentrations.

An imaging fibre that contained three different sensing regions was fabricated for simultaneous measurements of O_2, pH and CO_2.[34] Each sensing region was photopolymerised as discrete sites on the end of a single fibre bundle (Figure 4b). The pH and oxygen sensor chemistry has been described above. The oxygen-sensing region was initially polymerised without the ruthenium dye, followed by exposure to a dye/solvent solution that infuses the dye into the polymer. This fabrication method avoids potential dye photobleaching in the photoinitiation step. Preparing the oxygen sensor first avoids exposing the other sensing regions to the ruthenium dye. The carbon dioxide sensor was prepared by immobilizing a fluorescein derivative in a polymer matrix, identical to the pH sensing regions. The polymer region was then saturated with a bicarbonate buffer solution and coated with a hydrophobic polymer. As carbon dioxide crosses this hydrophobic membrane, the pH decreases due to the carbonic acid reaction, resulting in a decreased fluorescence response from the interior pH sensitive region. In this fashion, the pH and CO_2 are both measured using the ratiometric method. All three sensors are reversible, and the CO_2 sensor is unresponsive to changing oxygen concentrations. This triple sensor was used for monitoring beer fermentation. Prior to the addition of yeast, all analyte levels remained constant. Upon yeast addition, all three sensors immediately responded as glucose was partially oxidized to carbon dioxide, oxygen was consumed and the pH decreased (Figure 12).

4.4.1 Oligonucleotide detection. Nucleic acids have inherent base-pair recognition capabilities that can be implemented as detection elements. Oligonucleotide recognition capabilities were first combined with electrophoretic gels for radiolabeled detection via the Southern method.[35] Fibre optic platforms now serve as a novel platform for fluorescence-based oligonucleotide detection.[8,36–43] Oligonucleotide sequences can be aligned directly with individual fibres in a fibre bundle, allowing parallel, high throughput analysis of genomic samples. The immobilized single-stranded sequences, or probes, are capable of recognizing their complementary sequence counterparts, or targets, from a complex solution. Because optical fibres are amenable to fluorescence-based techniques, combining single-stranded oligonucleotides with optical fibres allows fluorescence-based methods to be used in place of the once standard radiolabel detection. A number of methods exist that can incorporate fluorescence into the probe-target pair. Fluorescence can be integrated directly into the target sequence via the polymerase chain reaction (PCR). PCR methods incorporate a fluorescence label either from fluorescent nucleotides or via fluorescently-labelled primer sequences used to initiate the PCR reaction, resulting in fluorescently-labelled, amplified target

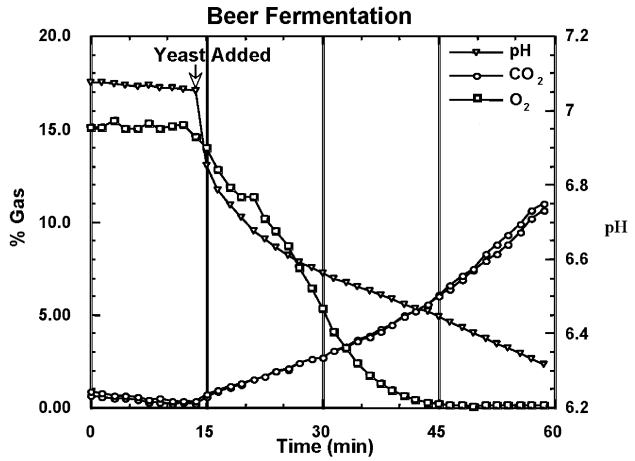

Fig. 12 Sensor responses for pH, O_2 and CO_2 sensors monitoring beer fermentation. Response changes occurred after the addition of yeast. Sensor reproducibility is demonstrated by the identical CO_2 curves from two CO_2 sensors in the array. Reprinted from "Simultaneous monitoring of pH, CO_2, and O_2 using an optical imaging fiber", J. A. Ferguson *et al*., Anal. Chim. Acta, 1997, **340**, 123, © 1997 with permission from Elsevier Science.

species. The PCR amplification process can also be used to concentrate specific mRNA transcripts from a complex sample, allowing transcripts of known importance to be identified. This method has become standard, and is important when sample amplification is necessary for detection. This labelled primer method can also be employed for reverse transcription (RT) assays to form cDNA (DNA complementary to mRNA transcripts that are being measured) while retaining their relative expression levels in the tissue. The cDNA formed in the RT process is also more stable than the transcript mRNA. Other methods exist to incorporate fluorescent dyes into nucleic acids, such as intercalating dyes or fluorescence resonance energy transfer (FRET) methods. Intercalating dyes bind to double stranded DNA, providing signal after the oligonucleotide duplex is formed. FRET methodology is a distance dependent fluorescence quenching method that will be described later under the molecular beacons section. In each case, correct probe-target hybridisation generates a fluorescence response. Fluorescence-based assays are extremely sensitive, and duplex formation can be controlled to interrogate single base differences, which can serve as important markers for genomic comparison or known genetic variations.

As with the artificial olfaction sensors, the first generation of oligonucleotide sensors involved polymeric sensing regions.[37,38] Single-stranded oligonucleotide probe sequences were attached to discrete photopolymerised regions on an imaging fibre's distal face.[38] The array was capable of demonstrating single base discrimination, and could interrogate submicrolitre sample volumes. Since DNA duplexes have a specific melting temperatures associated with dissociation, the probe-target pairs could be denatured, restoring the oligonucleotide probes to their single-stranded forms for reuse. This oligonucleotide array was regenerated with elevated temperature and repeated on the same fibre for three consecutive assays. Oligonucleotide arrays could also be fabricated on single core fibres (200 μm diameter). The ssDNA probes were coupled directly to a polymer covering the fibre cores.[37] Multiple single core fibres were then bundled to provide a parallel detection scheme. The bundled array demonstrated the ability to profile gene products amplified via PCR. This scheme also enabled the detection of unlabeled target molecules. The oligonucleotide arrays were first exposed to fluorescently-labelled synthetic targets that hybridised with the ssDNA, supplying the array with an initial fluorescent signal. The unlabeled target sample was then hybridised to the same array to displace the pre-hybridised fluorescent species, resulting in a fluorescence decrease. The fluorescence decrease was proportional to increasing concentrations of the unlabeled sample target solutions. The probes were regenerated by exposure to organic denaturants or elevated temperatures. These assays provided a rapid, reusable platform for oligonucleotide detection.

4.4.2 High-density microsphere-based oligonucleotide arrays. The magnitude and complexity of the human genome epitomize the need for nucleic acid detection technology that is rapid and efficient at detecting a large number of genetic differences. Array platforms have advanced the reproducibility and consistency of large-scale nucleic acid detection by enabling high throughput parallel analysis. Typical oligonucleotide microarrays use thousands of gridded microscopic single-stranded (ss) DNA spots arranged on a solid substrate, and as such, are platforms suitable for simultaneous genetic analysis of a complex target solution. For example, many molecular events are dependent on a cluster of genes or a series of gene networks. The expression profile of diseased tissue could be matched against healthy control tissue to determine relevant gene transcripts that are differentially (up- or down-) regulated. The target DNA from the two different tissue samples can be labelled with different fluorescent dyes to compare the hybridisation ratios.[44] The extent of hybridisation generates signals that relate directly to the abundance, or expression level, of each transcript. The concept of a gridded ssDNA array has developed into a number of notable platforms over the last decade, including those fabricated by ink-jet deposition[45] and photolithography.[46,47] Comprehensive reviews of fluorescence-based nucleic acid detection and microarrays have recently been published.[2,44]

The second generation of fibre optic DNA arrays incorporated microsphere sensors as the individual sensing elements.[8,9,36] The principle is similar to the described microsphere arrays used in artificial olfaction, except the sensing elements are ssDNA probe sequences attached to the microsphere surface. As described above, billions of identical sensors can be made simultaneously.[7–9] Microsphere encoding is required for positional registration and enables the user to differentiate large numbers of different DNA probe types in the microwell array.

While this fibre optic microsphere-based array platform is comparable to other DNA array detection schemes, it has a few major advantages. The platform is regenerable, with the ability to use a single array for dozens of assays while many other arrays can be used only once. This platform has a simple, flexible fabrication protocol. The fabrication process allows customizing the numbers of sensors in the array. Greater numbers of identical sensors can be added to improve the signal-to-noise ratio and offset the occurrence of false positive and false negative signals. As new sequences of interest are discovered, they can be attached to microspheres and added to the existing sensor pool to be incorporated into new arrays. This microsphere-based platform has the smallest element sizes (3 μm) of any array format, which provides a greater sensor packing density ($\sim 2 \times 10^7$ microsphere sensors per cm^2) and smaller overall feature sizes. By keeping the overall dimensions of the array extremely small, smaller volumes of sample are needed. DNA hybridisations are diffusion dependent, so the same number of target molecules in a smaller volume yields a more rapid response, increasing the experimental throughput. The miniature feature sizes also provide a detection advantage. By confining target molecules to a small volume, a high local concentration is achieved. For example, a few hundred target molecules confined to a 3 μm well of approximately 30 femtolitres volume relates to nanomolar concentration. Nanomolar concentrations are readily detectable using fluorescence. The next several sections will describe the use of the imaging fibre microwell array as a unique platform for oligonucleotide-based assays.

Multiplexed arrays were used with twenty-five different microsphere-types to detect different cystic fibrosis mutations and cytokines.[8] The arrays could monitor hybridisations in real time, and nanomolar concentration hybridisations could be detected within a few seconds. A single array was reused over 100 times with minimal signal differences between hybridisations, and array regeneration was completed upon 1 second exposures to denaturants.

Additional experiments were performed to determine the array's detection limits.[36] The number of microsensors in the arrays have a dramatic effect on the detection limits, which can be controlled to suit the experiment (Figure 13). As with the artificial nose, greater numbers of identical microsensors provide a signal-to-noise (S/N) advantage, increasing the S/N ratio based on the number of identical sensors in the array. Conversely, fewer sensors provide a numerical advantage because as hybridisation goes to completion, the same absolute number of target molecules hybridised to fewer microspheres would provide more target molecules per microsphere and a higher, more easily detected signal. This concept has enabled a zeptomole detection limit (~600 molecules), the lowest detection limit of any array platform. Experiments were performed with a 10^9-fold excess of irrelevant DNA without affecting the detection limits. Other methods to detect such small total target molecule numbers require lasers and confocal optics, while the fibre array system employs a white light source and CCD camera.

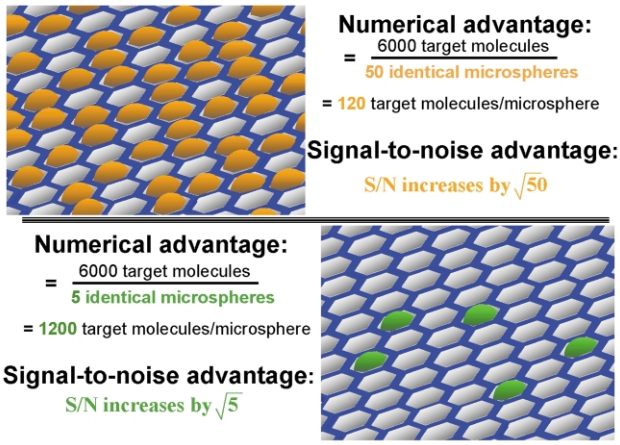

Fig. 13 The effects of increasing numbers of microspheres in the array.

The third generation of DNA microarrays developed with the fibre optic platform also employs microsphere-based sensing elements, but with a modified DNA detection methodology. The microsphere-based array platform has been combined with both molecular beacons[40] and aptamers.[39] Both schemes utilize the inherent recognition capabilities of nucleic acids, but take advantage of a nucleic acid sequences' ability to adopt different three-dimensional conformations.

4.4.3 Molecular beacons. Fluorescence resonance energy transfer (FRET) is a technique incorporated into the fibre optic sensor array platform for detection of unlabeled target molecules.[40,48] FRET uses a donor fluorophore coupled to an acceptor chromophore. The efficiency of donor to acceptor energy transfer is determined by their separation distance and spectral overlap. When the donor and acceptor are proximal, the acceptor reduces the donor fluorescence by one of two methods. First, an acceptor can be a quenching molecule, designed to non-radiatively stifle the donor fluorescence. Second, the acceptor can possess an excitation band overlapping the donor's emission wavelength. In this instance, the excited donor fluorophore is returned to the ground state and its energy is transferred to the acceptor emission. This donor/acceptor FRET design has been combined with nucleic acid probe sequences for molecular beacon sensor arrays.

Molecular beacons tether the donor and acceptor molecules to opposite termini of a single-stranded oligonucleotide probe sequence. The oligonucleotide sequence consists of a recognition segment, flanked by short complementary ends. In the absence of a target complementary to the recognition sequence, the two flanking sequences hybridise to form a stem-loop structure (Figure 14a). This conformation brings the donor and acceptor in proximity and the donor's fluorescence is reduced. Binding between the molecular beacon recognition segment and its correct single-stranded target, unfolds the stem-loop structure and spatially separates the donor and acceptor. This separation allows the donor signal to fluoresce uninhibited (Figure 14b), and signals the presence of the complementary oligonucleotide target.

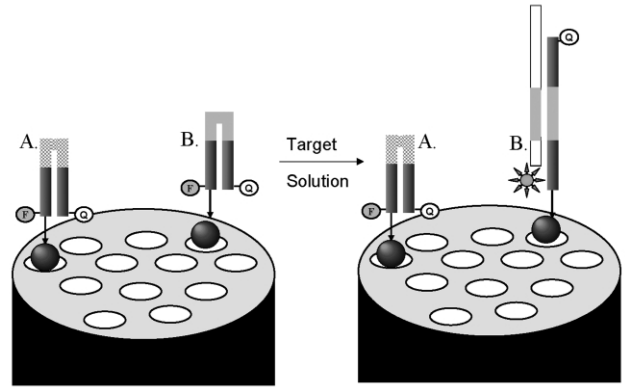

Fig. 14 Molecular beacons. In the absence of target molecules complementary to the loop structures, the beacons remain in a hairpin formation, the fluorophore (F) and quencher (Q) remain close, and fluorescence is quenched. Upon complementary target binding, the beacon opens, allowing F to fluoresce uninhibited.

Fibre optic microarrays utilizing molecular beacons were used for label-less detection of cystic fibrosis gene targets.[40] Fluorescein and 4-(4-dimethylaminophenylazo)benzoic acid were employed as the fluorophore and quencher respectively. The molecular beacon arrays provided a rapid response capable of quantitative measurements of target solutions. This platform is regenerable and has a picomolar detection limit. Label-less detection provides a simpler, faster protocol that can analyse unpurified solutions, limiting excessive sample manipulation, without the need for extra sample handling necessary for PCR-based label incorporation.

4.4.4 Aptamers. Aptamers are nucleic acid recognition sequences selected from a random library based on direct interaction with a target molecule or protein.[49,50] Aptamer development involves successive cycles of screening a combinatorial aptamer library followed by enrichment for those sequences exhibiting the desirable binding characteristics. The binding characteristics are based on each aptamer's unique three-dimensional structure. The aptamer library is exposed to target molecules tethered to a solid support, binding those with the preferred interactions, while any non-interacting sequences are washed away. The retained sequences are isolated, amplified and subjected to successive screening cycles of increasing stringency. In this manner, only those few candidates with the greatest affinity for the target molecule are selectively enriched.

Nucleic acid aptamers are natural choices for recognition elements because they are selected to interact with specific target molecules. Targets to which aptamers have been selected include small proteins or other similar sized molecular species, with binding monitored via techniques such as surface plasmon resonance[51] or absorbance spectroscopy coupled with capillary

electrophoresis.[52,53] A fibre optic microarray was fabricated with aptamers specific for thrombin, an important biomolecule in blood clotting.[39] Aptamer arrays provide quantitative signal responses to fluorescently-labelled target solutions. Detection of unlabeled target samples is preferable because labelling samples requires additional labour. Unlabeled thrombin also was detected down to 1 nanomolar concentrations in a competitive assay similar to the general microsphere-based DNA method described above. The arrays were reusable over multiple assays, with assays completed in 15 minutes, including regeneration of the array.

5 Cell-based microarrays

Fibre optic arrays can also employ living cells as the sensing elements positioned in the etched fibre wells (Figure 15). Cell-based arrays provide a unique sensing method compared to other multiplexed sensing schemes, because live cells can respond to a wide variety of biologically significant compounds. Cell responses are either physiological or genetic. Physiological responses are based on local environmental changes such as pH, O_2 and CO_2. Genetic responses link a promoter gene with an adjacent reporter gene that codes for an optically detectable biomolecule. The biomolecule's signal response corresponds to the promoter's expression level. The promoter's expression can be affected by multiple parameters, including environmental conditions and cellular metabolic processes that regulate (up- or down-) promoter expression. Because the promoter is linked to the reporter gene, the fluorescence response correlates to the conditions that affect the promoter activity.

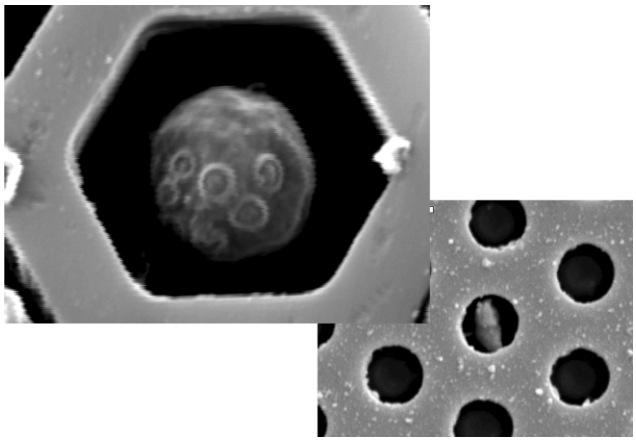

Fig. 15 Cells in wells. The microwells can be tailored to match the size of different cells, including yeast (left) and bacteria (right). Reprinted with permission from I. Biran and D. R. Walt, *Anal. Chem.*, 2002, **74**, 3046. © 2002 American Chemical Society.

While many other cell-based assays are limited by the accuracy and reproducibility of the analytical measurements, the optical fibre platform allows non-invasive, repetitive measurements of thousands of individual live cells simultaneously. This platform provides a simple indexing, mapping, and fabrication protocol, and once fabricated, an array does not require manual sample manipulation. Because cells localize randomly into the etched microwells, they are encoded with dyes to positionally register each specific cell type. By employing several dyes or dye ratios, multiple different cell lines/strains can be addressed in parallel, further increasing the experimental complexity in a simple, directed manner. The cell responses can be measured individually, or as an average response. Interrogating each cell individually is beneficial because each cell has a different metabolic rate and is at a different stage of its life cycle. Cell viability is not compromised, and neither physical indexing nor sequential scanning are required. Experimental reproducibility can be validated with cell replicates in the array. A single assay can provide a massive amount of information and can be used for high throughput screening (HTS) drug discovery applications.

Initial fibre optic cell-array research employed mouse fibroblast NIH 3T3 cells as the sensing elements located in the microwell array.[6] Cells were encoded via standard lipophilic dye kits, allowing the dye to passively diffuse into the cell membrane. The encoding dyes are not cytotoxic and are rapidly incorporated into the cells. The cells adhere to the well bottoms, and are positionally mapped via their internal dyes. Cell viability is confirmed with standard Live/Dead assay kits. These kits demonstrate cell viability based on non-specific enzyme processes and membrane permeability. For live cells, dye precursors diffuse into the cell interior and are converted to fluorescent species by non-specific enzyme processing. In this case, the generation of a fluorescent signal indicates cell viability. Fluorescent indicators that denote dead cells, such as DNA intercalators, are unable to permeate intact cell membranes and do not provide a signal for live cells. Non-viable cells have compromised membranes that allow these dyes to intercalate with the cellular DNA and generate a signal indicative of cell death.

These types of cell arrays were used to measure cell metabolism based on extracellular pH changes. Arrays were combined with 100 nm sized particles embedded with a pH-sensitive fluorescent dye. The nanoparticles were immobilized in a polymer layer at the bottom of the microwells before loading the array with cells and were incapable of reaching the cell interior. The nanoparticles were added in concentrations such that numerous nanoparticles accumulated in each well. The microwells containing individual cells exhibited a fluorescence decrease as cell metabolism leads to an extracellular pH decrease. Nanoparticles occupying wells without cells did not exhibit any fluorescence change. This pH sensitive cell array system is capable of measuring cell responses affected by O_2, CO_2 and glucose, among others.

A second generation of cell arrays utilized an advanced encoding strategy.[5] Concanavalin A was conjugated to multiple fluorescent dyes that were used to encode yeast cells (*S. cerevisiae*) via binding to mannoproteins present on the cell wall. This methodology could also be used for other available surface protein/fluorescent dye pairs. Bacterial cells (*E. coli*) can also be engineered to express different fluorescent proteins that can be employed for encoding. Plasmids encoding naturally fluorescent biomolecules, such as green fluorescent protein and its variants, were incorporated into the cells. Experiments were performed using three different optically detectable proteins, but the potential exists to scale up the number of unique genetic encoding signatures by using other combinations of commercially available plasmids.

This second generation of cell-based array assays was developed taking advantage of cell-engineering techniques. Engineered yeast cells containing the reporter *lacZ* gene coding for the enzyme β-galactosidase were used. β-galactosidase is not an optically detectable species, but processes a precursor substrate added to the medium into a fluorescent molecular signal. The yeast cells utilized the *lacZ* reporter gene expression in combination with a known two-hybrid system. Two hybrid systems regulate their reporter response on the basis of specific protein–protein interactions. The extent to which the two proteins interact affects the transcription level of the reporter gene, which mediates the fluorescent response. The two proteins are introduced into the cell via plasmids; a binding domain encoding one protein and an activating domain in a second plasmid. When the two coded proteins interact, a transcription factor complex is activated, initiating transcription of the reporter gene downstream of the binding site. For these cell-based assays, the two-hybrid system was based on the

interaction of large T-antigen proteins, p53 and SV40. Three cell strains were investigated; a positive strain expressing the correct hybrid pair, a negative strain expressing non-interacting proteins, and a wild type strain without the two-hybrid system. The majority of positive responses were linked to the positive strain, with a few negative strains also exhibiting a fluorescence increase. The wild type strains did not exhibit any fluorescence response.

This cell-array platform can provide a rapid, repetitive analysis of live cell metabolic responses, and is a valuable tool for HTS. The miniature array size enables interrogation of smaller volumes with lower reagent costs, often a concern in cell-based HTS processes. Arrays can also be patterned into a 96- or 384- matrix. The matrix positions can then be paired with the wells of microtitre plates, such that multiple identical arrays can be screened in a microtiter plate format simultaneously, further increasing the throughput.

6 Conclusions

Fibre optic imaging bundles are a universal sensing platform capable of numerous sensing schemes, ranging from relatively simple pH sensors, to high-throughput cell-based screening. Imaging fibres enable combined imaging and sensing that relates physical changes with responses monitored by the sensor. Fibre optic imaging arrays possess miniature feature sizes, allowing high-density sensor packing ($\sim 2 \times 10^7$ sensors per cm^2). The miniature feature sizes enable a fast response and more sensitive measurement capabilities. The platform's versatility in experimental design is exemplified by the multiple methods developed for fabricating sensing regions. The array platform can be tailored to suit the experimental design, whether it is for monitoring single analytes or for more complex assays, including artificial olfaction, DNA detection, or cell-based screening. While a number of schemes have been described in this review, the indicators or other parameters can be adapted to suit other sensing designs, allowing these array formats to be further exploited for other specific applications.

7 References

1 O. S. Wolfbeis, *Anal. Chem.*, 2002, **74**, 2663.
2 J. R. Epstein, I. Biran and D. R. Walt, *Anal. Chim. Acta*, 2002, **469**, 3.
3 J. White, J. S. Kauer, T. A. Dickinson and D. R. Walt, *Anal. Chem.*, 1996, **68**, 2191.
4 P. Pantano and D. R. Walt, *Chem. Mater.*, 1996, **8**, 2832.
5 I. Biran and D. R. Walt, *Anal. Chem.*, 2002, **74**, 3046.
6 L. C. Taylor and D. R. Walt, *Anal. Biochem.*, 2000, **278**, 1242.
7 K. L. Michael, L. C. Taylor, S. L. Schultz and D. R. Walt, *Anal. Chem.*, 1998, **70**, 1242.
8 J. A. Ferguson, F. J. Steemers and D. R. Walt, *Anal. Chem.*, 2000, **72**, 5618.
9 D. R. Walt, *Science*, 2000, **287**, 451.
10 K. L. Michael and D. R. Walt, *Anal. Biochem.*, 1999, **273**, 168.
11 A. A. Panova, P. Pantano and D. R. Walt, *Anal. Chem.*, 1997, **69**, 1635.
12 S. Szunerits and D. R. Walt, *Anal. Chem.*, 2002, **74**, 886.
13 B. G. Healey and D. R. Walt, *Anal. Chem.*, 1997, **69**, 2213.
14 S. M. Barnard and D. R. Walt, *Nature*, 1991, **353**, 338.
15 J. S. Kauer, *Trends Neurosci.*, 1991, **14**, 79.
16 T. A. Dickinson, J. White, J. S. Kauer and D. R. Walt, *Nature*, 1996, **382**, 697.
17 T. A. Dickinson, D. R. Walt, J. White and J. S. Kauer, *Anal. Chem.*, 1997, **69**, 3413.
18 S. R. Johnson, J. M. Sutter, H. L. Engelhardt, P. C. Jurs, J. White, J. S. Kauer, T. A. Dickinson and D. R. Walt, *Anal. Chem.*, 1997, **69**, 4641.
19 T. A. Dickinson, K. L. Michael, J. S. Kauer and D. R. Walt, *Anal. Chem.*, 1999, **71**, 2192.
20 K. J. Albert, D. R. Walt, D. S. Gill and T. C. Pearce, *Anal. Chem.*, 2001, **73**, 2501.
21 K. J. Albert and D. R. Walt, *Anal. Chem.*, 2000, **72**, 1947.
22 S. E. Stitzel, L. J. Cowen, K. J. Albert and D. R. Walt, *Anal. Chem.*, 2001, **73**, 5266.
23 J. W. Gardner and P. N. Bartlett, *Electronic Noses: Principles and Applications*, Oxford University Press, Cambridge, 1999.
24 J. W. Gardner and P. N. Bartlett, *Sens. Actuators, A*, 1995, **A51**, 57.
25 M. C. Burl, B. C. Sisk, T. P. Vaid and N. S. Lewis, *Sens. Actuators, B*, 2002, **B87**, 130.
26 J. W. Grate, S. L. Rose-Pehrsson, D. L. Venezky, M. Klusty and H. Wohltjen, *Anal. Chem.*, 1993, **65**, 1868.
27 J. W. Grate and B. M. Wise, *Anal. Chem.*, 2001, **73**, 2239.
28 M. C. Lonergan, E. J. Severin, B. J. Doleman, S. A. Beaber, R. H. Grubbs and N. S. Lewis, *Chem. Mater.*, 1996, **8**, 2298.
29 J. R. Stetter, P. C. Jurs and S. L. Rose, *Anal. Chem.*, 1986, **58**, 860.
30 L. B. Buck, *Annu. Rev. Neurosci.*, 1996, **19**, 517.
31 K. S. Bronk, K. L. Michael, P. Pantano and D. R. Walt, *Anal. Chem.*, 1995, **67**, 2750.
32 B. G. Healey and D. R. Walt, *Anal. Chem.*, 1995, **67**, 4471.
33 L. Li and D. R. Walt, *Anal. Chem.*, 1995, **67**, 3746.
34 J. A. Ferguson, B. G. Healey, K. S. Bronk, S. M. Barnard and D. R. Walt, *Anal. Chim. Acta*, 1997, **340**, 123.
35 E. M. Southern, *J. Mol. Biol.*, 1975, **98**, 503.
36 J. R. Epstein, M. Lee and D. R. Walt, *Anal. Chem.*, 2002, **74**, 1836.
37 J. A. Ferguson, T. C. Boles, C. P. Adams and D. R. Walt, *Nat. Biotechnol.*, 1996, **14**, 1681.
38 B. G. Healey, R. S. Matson and D. R. Walt, *Anal. Biochem.*, 1997, **251**, 270.
39 M. Lee and D. R. Walt, *Anal. Biochem.*, 2000, **282**, 142.
40 F. J. Steemers, J. A. Ferguson and D. R. Walt, *Nat. Biotechnol.*, 2000, **18**, 91.
41 J. M. Yeakley, J.-B. Fan, D. Doucet, L. Luo, E. Wickham, Z. Ye, M. S. Chee and X.-D. Fu, *Nature Biotechnol.*, 2002, **20**, 353.
42 P. A. E. Piunno, U. J. Krull, R. H. E. Hudson, M. J. Damha and H. Cohen, *Anal. Chem.*, 1995, **67**, 2635.
43 A. P. Abel, M. G. Weller, G. L. Duveneck, M. Ehrat and H. M. Widmer, *Anal. Chem.*, 1996, **68**, 2905.
44 D. J. Lockhart and E. A. Winzeler, *Nature*, 2000, **405**, 827.
45 T. R. Hughes, M. Mao, A. R. Jones, J. Burchard, M. J. Marton, K. W. Shannon, S. M. Lefkowitz, M. Ziman, J. M. Schelter, M. R. Meyer, S. Kobayashi, C. Davis, H. Dai, Y. D. He, S. B. Stephaniants, G. Cavet, W. L. Walker, A. West, E. Coffey, D. D. Shoemaker, R. Stoughton, A. P. Blanchard, S. H. Friend and P. S. Linsley, *Nat. Biotechnol.*, 2001, **19**, 342.
46 S. P. A. Fodor, J. L. Read, M. C. Pirrung, L. Stryer, A. T. Lu and D. Solas, *Science*, 1991, **251**, 767.
47 J. A. Warrington, N. A. Shah, X. Chen, M. Janis, C. Liu, S. Kondapalli, V. Reyes, M. P. Savage, Z. Zhang, R. Watts, M. DeGuzman, A. Berno, J. Snyder and J. Baid, *Human Mutation*, 2002, **19**, 402.
48 S. Tyagi and F. R. Kramer, *Nat. Biotechnol.*, 1996, **14**, 303.
49 A. D. Ellington and J. W. Szostak, *Nature*, 1992, **355**, 850.
50 C. Tuerk and L. Gold, *Science*, 1990, **249**, 505–10.
51 F. Darfeuille, A. Arzumanov, S. Gryaznov, M. J. Gait, C. Di Primo and J.-J. Toulme, *Proc. Natl. Acad. Sci. U. S. A.*, 2002, **99**, 9709.
52 V. Pavski and X. C. Le, *Anal. Chem.*, 2001, **73**, 6070.
53 J. A. M. Charles and L. B. McGown, *Electrophoresis*, 2002, **23**, 1599.